The Pharmacogenomics Journal (2013), 1–7

www.nature.com/tpj

ORIGINAL ARTICLE

High warfarin sensitivity in carriers of *CYP2C9*35* is determined by the impaired interaction with P450 oxidoreductase

M-Y Lee[1], P Borgiani[2], I Johansson[1], F Oteri[3], S Mkrtchian[1], M Falconi[3] and M Ingelman-Sundberg[1]

Cytochrome P450 2C9 (CYP2C9) metabolizes many clinically important drugs including warfarin and diclofenac. We have recently reported a new allelic variant, *CYP2C9*35*, found in a warfarin hypersensitive patient with Arg125Leu and Arg144Cys mutations. Here, we have investigated the molecular basis for the functional consequences of these polymorphic changes. CYP2C9.1 and CYP2C9-Arg144Cys expressed in human embryonic kidney 293 cells effectively metabolized both *S*-warfarin and diclofenac in NADPH-dependent reactions, whereas CYP2C9-Arg125Leu or CYP2C9.35 were catalytically silent. However, when NADPH was replaced by a direct electron donor to CYPs, cumene hydroperoxide, hereby bypassing the CYP oxidoreductase (POR), all variant enzymes were active, indicating unproductive interactions between CYP2C9.35 and POR. *In silico* analysis revealed a decrease of the electrostatic potential of CYP2C9-Arg125Leu-POR interacting surface and the loss of stabilizing salt bridges between these proteins. In conclusion, our data strongly suggest that the Arg125Leu mutation in CYP2C9.35 prevents CYP2C9-POR interactions resulting in the absence of NADPH-dependent CYP2C9-catalyzed activity *in vivo*, thus influencing the warfarin sensitivity in the carriers of this allele.

The Pharmacogenomics Journal advance online publication, 10 December 2013; doi:10.1038/tpj.2013.41

Keywords: cytochrome P450 2C9; *CYP2C9*35*; diclofenac; P450 oxidoreductase; structural modeling; warfarin

INTRODUCTION

Cytochrome P450s (CYPs) are heme-containing enzymes that play important roles in the conversion of many xenobiotics and endogenous compounds into the corresponding hydroxylated metabolites. The reducing equivalents used in such enzymatic reactions are supplied by NADPH via CYP oxidoreductase (POR),[1] which directly interacts with CYPs. In addition to NADPH, certain organic hydroperoxides can also support the CYP-dependent hydroxylation of various drugs and fatty acids in the peroxidase-type reaction, bypassing POR as an electron carrier.[2] This peroxide-dependent pathway is known as a 'peroxide shunt'.[3]

The CYP2C subfamily accounts for about 18% of total CYP proteins in human liver microsomes.[4] CYP2C9 is one of the most abundant CYP enzymes in the liver responsible for approximately 12.8% of the metabolism of clinically important drugs including warfarin, losartan and diclofenac.[5] Warfarin is a worldwide prescribed anticoagulant, largely utilized for long-term treatment and prevention of thromboembolic events. However, warfarin treatment needs a constant clinical follow-up because of its narrow therapeutic range and high interindividual variability in the drug dose required for the therapeutic effect. This variability is thought to be dependent on both environmental and genetic factors, with the latter having an important role.[6]

CYP2C9 has been demonstrated to be polymorphic in several populations. Frequencies of variant CYP2C9 alleles in Caucasian are about 17% for *CYP2C9*2* (characterized by a Arg144Cys amino-acid change) and 6% for *CYP2C9*3* (Ile359Leu).[5] Both homozygote and heterozygote carriers of these two variants have been shown to have altered drug metabolism, for example, reduced warfarin clearance and lower daily dose requirement.[7,8] The *CYP2C9*2* and **3* variant alleles cause significantly decreased activity toward many other drugs, such as diclofenac,[9] losartan[10] and others.[11,12]

The molecular and structural basis for altered catalytic properties of polymorphic CYP enzyme variants is often poorly studied. However, the recent advances in resolution of three-dimensional structures of many CYPs including CYP2C9[13,14] allowed the development of various computational approaches that are currently applied for quantitative prediction of pharmacokinetics, interaction between the enzyme and its substrates, and also redox partners.[15–19] Thus, molecular dynamic simulations and subsequent substrate-docking simulations have been performed to clarify the mechanisms of enzymatic activity decrease in the different allelic variants of CYP2C9.[20] Amino-acid substitutions in these proteins were found to increase the fluctuation of the residues responsible for the substrate holding and alteration of the substrate-binding pocket.[20]

Recently, we have described warfarin hypersensitivity in one Italian patient at the Centre of Haemostasis and Thrombosis of PTV (Policlinico Tor Vergata, Rome, Italy), who required only 2.25 mg warfarin per week to achieve therapeutic anticoagulation effect, a dose that is substantially below the normal prescription range.[21] Sequencing of genes encoding enzymes involved in warfarin metabolism revealed a novel CYP2C9 allele designated as *CYP2C9*35* (http://www.cypalleles.ki.se/). It represents a novel CYP2C9 variant carrying the Arg144Cys substitution present in *CYP2C9*2* allele, and in addition also an Arg125Leu substitution.[21] *In silico* analysis suggested that Arg125Leu substitution might cause reduction of the positive potential of CYP2C9-POR interaction surface preventing the POR recognition, and negatively affecting the CYP2C9 activity toward warfarin.[21]

[1]Section of Pharmacogenetics, Department of Physiology and Pharmacology, Karolinska Institutet, Stockholm, Sweden; [2]Department of Biomedicine and Prevention, Genetics Unit, University of Rome 'Tor Vergata', Rome, Italy and [3]Department of Biology, University of Rome 'Tor Vergata' and Interuniversity Consortium, National Institute Biostructures and Biosystems (INBB), Rome, Italy. Correspondence: Associate Professor M Falconi, Department of Biology, University of Rome 'Tor Vergata' and Interuniversity Consortium, National Institute Biostructures and Biosystems (INBB), Rome, Italy or Professor M Ingelman-Sundberg, Section of Pharmacogenetics, Department of Physiology and Pharmacology, Karolinska Insittutet, Stockholm 171 77, Sweden.
E-mail: falconi@uniroma2.it or Magnus.Ingelman-Sundberg@ki.se
Received 15 May 2013; revised 1 November 2013; accepted 6 November 2013

The purpose of this study was to validate experimentally this hypothesis using *in vitro* cell system expressing several CYP2C9 variant enzymes in combination with extended structural bioinformatics analysis based on the crystal structure of CYP2C9. The data show complete abolition of NADPH-dependent hydroxylation of two CYP2C9 substrates, *S*-warfarin and diclofenac in human embryonic kidney 293 (HEK293) cells expressing CYP2C9-R125L, whereas the activity was recovered by direct CYP activation using CuOOH, compliant with ineffective CYP2C9-POR interactions as a main cause of abnormal warfarin hypersensitivity associated with the CYP2C9.35 variant.

MATERIALS AND METHODS

Chemicals and reagents

S-warfarin, 7′-hydroxywarfarin, diclofenac sodium salt, 4′-hydroxydiclofenac, cumene hydroperoxide, acetonitrile and phosphoric acid were obtained from Sigma-Aldrich (Sigma-Aldrich Sweden AB, Stockholm, Sweden). Losartan carboxylic acid (E-3174) was purchased from Santa Cruz Biotech (Dallas, TX, USA). QuikChange Lightning Site-Directed Mutagenesis Kit was purchased from Stratagene (La Jolla, CA, USA). HEK Flp-In™-293 cell line, Lipofectamine 2000 and cell medium were purchased from Invitrogen (Life Technologies Europe BV, Stockholm, Sweden). All solvents for high-performance liquid chromatography (HPLC) assay were obtained from Merck KGaA (Darmstadt, Germany).

Molecular cloning and site-directed mutagenesis

Human CYP2C9 cDNA was introduced into pcDNA™5/FRT, commercial Flp-In™ expression vector (Invitrogen), using restriction enzymes *Kpn*I and *Not*I. CYP2C9-R125L, CYP2C9-R144C (*CYP2C9*2*) and CYP2C9-R125L/R144C (*CYP2C9*35*) genetic variants were constructed from pcDNA5/FRT-CYP2C9 (*CYP2C9*1*) with a QuickChange Lightning Site-Directed Mutagenesis Kit (Stratagene). The mutations were introduced using mutagenic primers (mutations in bold), 5′-GGAAGGAGATCCGGC**T**TTTCTCCCTCATGACG-3′ for Arg125Leu (G374T) and 5′-GAGGAGCATTGAGG**A**C**T**GTGTTCAAGAGGAAGC-3′ for Arg144Cys (C430T). These variant cDNAs were subcloned and correct mutagenesis was confirmed by DNA sequencing.

Generation of stable CYP2C9 Flp-In™-293 cells

Following the manufacturer's guidelines, Flp-In™-293 cells were cultured in Dulbecco's modified Eagle's medium with 10% fetal bovine serum (Cat. no. 10106; Invitrogen), 100 U ml^{-1} penicillin–streptomycin and zeocin (100 μg ml^{-1}). Cells were transfected with pcDNA™5/FRT-CYP2C9 (*CYP2C9*1*), pcDNA™5/FRT-CYP2C9-R125L, pcDNA™5/FRT-CYP2C9-R144C (*CYP2C9*2*) and pcDNA™5/FRT-CYP2C9-R125L/R144C (*CYP2C9*35*) using Lipofectamine 2000. After 48 h, cells were selected by hygromycin B (75 μg ml^{-1}) in the complete Dulbecco's modified Eagle's medium containing 10% fetal bovine serum and 100 U ml^{-1} penicillin–streptomycin including 2 mM L-glutamine. Empty pcDNA™5/FRT was transfected in the same manner to produce mock-Flp-In™-293 cells as a negative control.

Western blot analysis

Total cell lysates were prepared using radio immunoprecipitation assay buffer (pH 8.0) (50 mM Tris-HCl, 150 mM NaCl, 1% NP-40, 0.5% sodium deoxycholate, 0.1% SDS, 0.5 mM EDTA) containing Complete Protease Inhibitor Cocktail (Roche Diagnostics, Mannheim, Germany) and total protein concentration was estimated by Bradford method.[22] Cell lysates or microsomes containing 20 μg of total protein were separated on 12% SDS-polyacrylamide gel and transferred to the nitrocellulose membrane (Hybond-C; Amersham Biosciences AB, Uppsala, Sweden). Membranes were probed with primary antibodies against CYP2C (α-hCYP2C, 1:1000; Edwards *et al.*[23]) and goat anti-rabbit secondary antibody conjugated to horseradish peroxidase (1:5000, Dako Cytomation, Glostrup, Denmark). Chemiluminescence was developed by SuperSignal West Pico (Pierce Chemical, Rockford, IL, USA) and visualized by the Fuji LAS 1000 (Fujifilm, Stockholm, Sweden) gel documentation system.

Isolation of microsomal fraction

Confluent cells from 150 mm dishes were washed with phosphate-buffered saline and scraped into eppendorf tubes. After centrifugation at 3000 r.p.m. in cold room for 5 min, the cell pellet was resuspended in 400 μl of buffer containing 20% glycerol, 1 mM EDTA, 10 mM Tris-HCl (pH 7.4), followed by sonication and centrifugation (9000 *g*, 20 min, 4 °C). The supernatant was centrifuged again at 105 000 *g* for 1 h (4 °C). The microsomal fraction pellet was resuspended in 50 mM potassium phosphate buffer (pH 7.4).

CYP2C9 mediated *S*-warfarin oxidation

Microsomes containing 300 μg of total protein were preincubated with different concentrations (0–40 μM) of *S*-warfarin in 10 mM potassium phosphate buffer (pH 7.4) at 37 °C for 5 min. The enzymatic reaction was initiated by adding 1 mM NADPH and carried on for 90 min at 37 °C in a total volume of 100 μl. The reaction rate was linear for up to 90 min. Alternatively, NADPH was substituted for cumene hydroperoxide (0.1–1 mM) and incubated with 10 μM of *S*-warfarin for up to 15 min. The reaction was stopped by adding 100 μl of ice-cold methanol containing E-3174, which was used as an internal standard for HPLC analysis.

After centrifugation at 17 000 *g* for 5 min, 30 μl of supernatant was injected into Zorbax 300SB-C18 (4.6 × 150 mm, 5 μm) column. HPLC analysis was carried out as in Lang and Bocker[24] with minor modifications. The mobile phase consisted of acetonitrile–1% phosphoric acid (38:62, v v^{-1}). The flow rate was 1 ml min^{-1}, fluorimetric detection at an excitation wavelength of 320 nm and an emission wavelength of 415 nm.[24,25] Spiked 7′-hydroxywarfarin, E-3174 and *S*-warfarin were eluted at 4.3, 5.5 and 8.3 min, respectively. The limit of detection was 18.99 pg (0.05 pmol) per injection. These data were further normalized by corresponding amounts of CYP2C9 variant proteins.

CYP2C9 mediated diclofenac oxidation

Microsomes containing 300 μg of total protein were preincubated with different concentrations (0–40 μM) of diclofenac in 10 mM potassium phosphate buffer (pH 7.4) at 37 °C for 5 min. The enzymatic reaction was initiated by adding 1 mM NADPH and carried on for 30 min at 37 °C in 100 μl of total reaction volume (diclofenac hydroxylation rate remained linear during this incubation period). Alternatively, NADPH was substituted for cumene hydroperoxide (0.1–1 mM) and reaction was carried on for up to 15 min in the presence of 10 μM diclofenac. The reaction was terminated by the addition of 20 μl of 30% acetonitrile containing internal standard and freezing in dry ice. Samples were acidified with 12 μl perchloric acid (0.5 M) and used further in the HPLC reverse phase system including Varian ProStar 310 UV–visible detector (UV 280 nm). After centrifugation (17 000 *g* for 10 min), 20 μl of acidified supernatant was injected into Zorbax 300SB-C18 (4.6 × 150 mm, 5 μm) column and separated using isocratic mobile phase (20 mM phosphoric acid (pH 2.1): acetonitrile (58:42)), flow rate, 1 ml min^{-1} (modified from Yasar *et al.*[9]). The peaks of diclofenac and its metabolite, 4′-hydroxydiclofenac were identified by spiking with standard compounds (Sigma). Quantification of 4′-hydroxydiclofenac (R_t = 4.3 min) was based on peak area measurements using linear calibration curves obtained with pure reference compounds and normalized by internal standard (*S*-warfarin, R_t = 5.5 min). The limit of detection was 1.03 pg (3.3 pmol) per injection of 4′-hydroxydiclofenac. These data were further normalized by the corresponding amounts of CYP2C9 variant proteins.

Data analysis

Apparent Michaelis–Menten constants K_m, V_{max} and intrinsic clearance (CL_{int}, V_{max}/K_m) were estimated by nonlinear regression analysis using Michaelis–Menten model (GraphPad Prism v.5.0; GraphPad Software, La Jolla, CA, USA). Statistical significance was assessed by using paired two-tailed *t*-test (GraphPad Prism).

Computational analysis: modeling of the CYP2C9 variant protein structures

The X-ray structure of the substrate-free CYP2C9 (PDB ID: 1OG2)[13] has been used as a template to model the structures of the Arg125Leu and Arg125Leu–Arg144Cys variants. The modeling procedure has been carried out using SYBYL 6.0 software (Tripos 1699, St Louis, MO, USA).

Modeling of the CYP–POR complex

The complex between the substrate-free CYP2C9 (PDB ID: 1OG2)[13] and the human flavine mononucleotide (FMN) binding domain (PDB ID: 1B1C)[26] of POR has been modeled using the corresponding complex from *Bacillus megaterium* (PDB ID: 1BVY) as a reference structural template.[27] The human FMN-binding domain of POR and CYP2C9 have been structurally aligned on the corresponding bacterial complex using the Matchmaker tool of the

UCSF Chimera program that constructs pairwise sequence alignments and uses them to superimpose the structures.[28] Residues that are located in the human complex interface have been identified using the NACCESS program,[29] calculating their solvent exposure both in the complex and in the isolated structures. The model interface has been refined using the HADDOCK docking program.[30]

Calculation of electrostatic potential

The atomic charges for the protein atoms have been assigned through the program PDB2PQR[31] using the AMBER force field.[32] The heme charges have been obtained from an *ad hoc* developed AMBER-compatible force field.[33] The electrostatic potential contour diagrams, calculated at 2.0*kT/e* for the CYP2C9.1 and variant proteins, have been obtained using the APBS (Advanced Poisson Boltzman Solver) free software,[34] applying the standard parameters (www.poissonboltzmann.org).

RESULTS

Generation of the stable Flp-In™-293 cells overexpressing CYP2C9.1, CYP2C9-R125L, CYP2C9-R144C and CYP2C9-R125L/R144C

CYP2C9.35 includes two amino-acid substitutions, Arg125Leu and Arg144Cys. To evaluate in detail their combined and individual effects on the catalytic activity, we have constructed FlpIn™-293 cell lines that stably express CYP2C9.1, CYP2C9.35, CYP2C9-R125L or CYP2C9-R144C (CYP2C9.2). All of these cell lines express approximately similar levels of CYP2C9 protein as measured by immunoblotting of the microsomal fraction isolated from these cells (Figure 1).

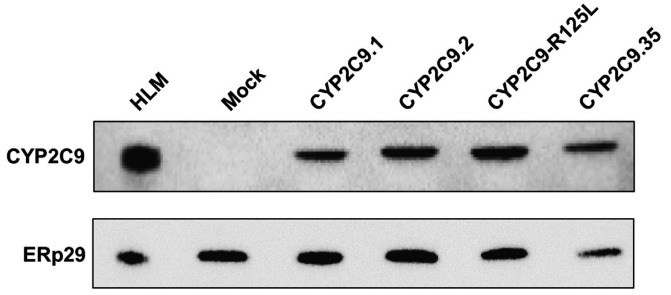

Figure 1. Western blot analysis of cytochrome P450 2C9 (CYP2C9) variant proteins' expression. Microsomes (20 μg of total protein) from transfected HEK Flp-In™-293 cells expressing CYP2C9 variant proteins were immunoblotted with anti-CYP2C and ERp29 antibodies[49] (immunodetection of ERp29 was used as a loading control because of the widespread and stable expression of ERp29 in all known cell types).[49] HLM, human liver microsomes (2 μg of total protein) were used as a positive control.

Hydroxylation of *S*-warfarin and diclofenac by CYP2C9 variants

To compare the catalytic activities of the different CYP2C9 variants, the microsomal fractions from HEK293 cells expressing CYP2C9.1, CYP2C9-R125L, CYP2C9-R144C (CYP2C9.2) and CYP2C9-R125L/R144C (CYP2C9.35) were incubated with *S*-warfarin and diclofenac in the presence of NADPH. Analysis by HPLC chromatography revealed that the enzymatic conversion of *S*-warfarin (Figure 2a and Supplementary Figure S1A) and diclofenac (Figure 2b and Supplementary Figure S2A) mediated by CYP2C9.1 and CYP2C9-R144C followed the Michaelis–Menten kinetics, which is in line with previously reported data.[9,11,12] However, the rate of both *S*-warfarin and diclofenac metabolism in the presence of CYP2C9 variants containing the Arg125Leu substitution, that is, CYP2C9-R125L and CYP2C9.35, was at the level of the background activity in the mock-transfected cells (Figure 2 and Supplementary Figures S1A and S2A). Identical results were obtained using yet another CYP2C9 substrate, losartan (results not shown).

Enzymatic activities of CYP2C9-R125L and CYP2C9.35 toward *S*-warfarin and diclofenac are recovered by replacing NADPH with cumene hydroperoxide

It has been suggested that the loss of CYP2C9.35 catalytic function is most probably connected with the weak interactions between CYP and POR rather than the impaired substrate binding.[21] To validate this hypothesis NADPH was replaced by CuOOH that can supply electrons to CYPs, circumventing POR ('peroxide shunt'[3]). The metabolism of both substrates in the presence of CuOOH was monitored for 15 min as longer incubations led to a sharp decline of enzymatic activity (Figure 3), apparently due to a rapid heme inactivation by CuOOH.[2,35] In line with previous reports,[12] we observed CYP2C9.1- and CYP2C9-R144C-dependent hydroxylation of *S*-warfarin to 7′-hydroxywarfarin in the presence of CuOOH similarly to NADPH-stimulated reaction. Strikingly, the same metabolite albeit at different levels was produced also in the

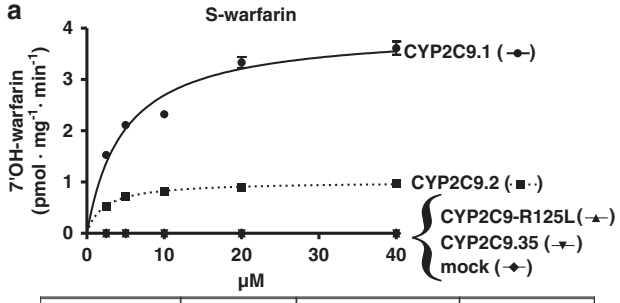

CYP2C9 variants	Km (μM)	Vmax (pmol • mg⁻¹ • min⁻¹)	CLint (Vmax/Km)
CYP2C9.1	4.76 ± 0.713	3.97 ± 0.177	0.839 ± 0.081
CYP2C9.2	2.20 ± 0.230	1.01 ± 0.023	0.463 ± 0.038
CYP2C9-R125L	-	-	-
CYP2C9.35	-	-	-

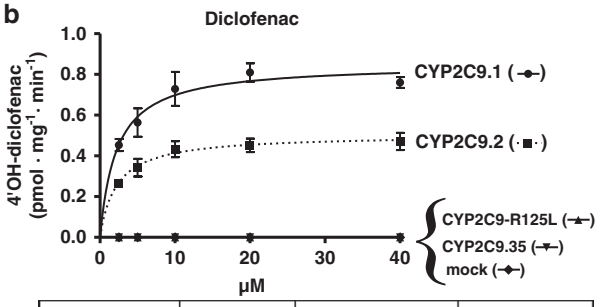

CYP2C9 variants	Km (μM)	Vmax (pmol • mg⁻¹ • min⁻¹)	CLint (Vmax/Km)
CYP2C9.1	2.19 ± 0.607	0.85 ± 0.05	0.414 ± 0.092
CYP2C9.2	2.20 ± 0.621	0.50 ± 0.03	0.243 ± 0.055
CYP2C9-R125L	-	-	-
CYP2C9.35	-	-	-

Figure 2. Nicotinamide adenine dinucleotide phosphate (NAPDH)-dependent hydroxylation of *S*-warfarin and diclofenac by the cytochrome P450 2C9 (CYP2C9) variant enzymes. Upper panel, Michaelis–Menten plots of 7′-hydroxywarfarin (**a**) and 4′-hydroxydiclofenac (**b**) formation in the presence of NADPH. Lower panel, the constants of enzymatic kinetics were calculated as it is described in Materials and Methods. The activity values were normalized by the corresponding amounts of CYP2C9 variant proteins estimated by densitometry of western blot bands (Image Gauge, v. 4.0; Fujifilm). All experiments were carried out in triplicates and the data are presented as mean ± s.e.m. '—', below the detection limit.

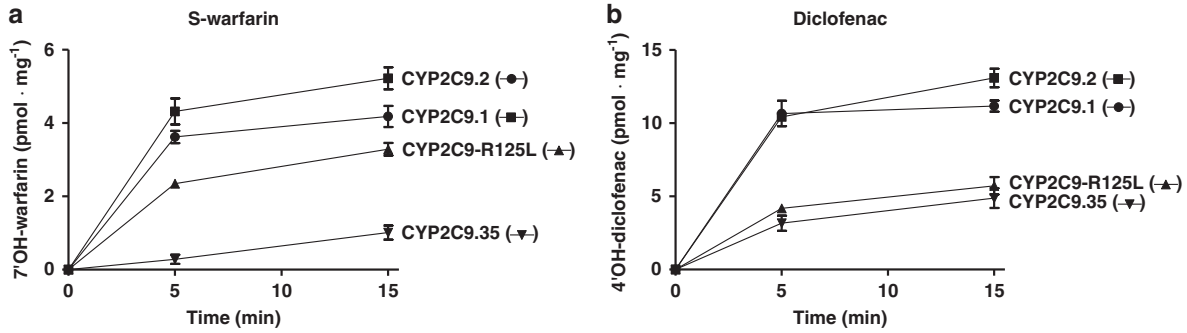

Figure 3. Cumene hydroperoxide-dependent metabolism of *S*-warfarin (**a**) and diclofenac (**b**) by cytochrome P450 2C9 (CYP2C9) variant enzymes. Activity values for *S*-warfarin (10 μM) and diclofenac (10 μM) metabolism with CuOOH (100 μM) were calculated as it is described in the Materials and Methods and normalized by the corresponding amounts of CYP2C9 variant enzymes (see legend to Figure 2). Experiments were performed in triplicates and the data are presented as mean ± s.e.m.

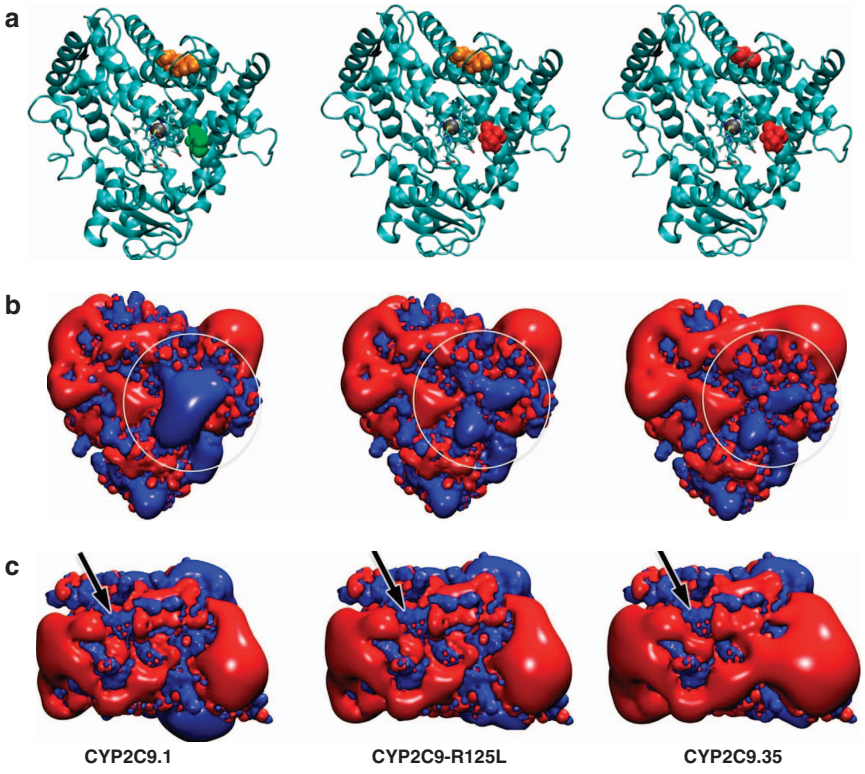

Figure 4. Modeling of equipotential electrostatic surface of cytochrome P450 2C9 (CYP2C9) variant proteins. (**a**) Protein structures are shown in cartoon representation with the heme group indicated by a gray ball-and-stick model. Arginines 125 and 144 are indicated by green and orange spacefill model, respectively. The mutated residues are colored in red. (**b**) Equipotential electrostatic surface of the region around the Arg125 has been enclosed by a white circle. Blue color indicates the positive isopotential surface at 2.0*kT/e* (*k*, Boltzmann constant, $T = 298$ K and $1kT/e = 0.0257$ V), whereas the red color shows the corresponding negative surface. (**c**) Equipotential electrostatic surface of the substrate access channel region of CYP2C9. The access channel entry has been indicated by a black arrow. The image was generated using the VMD (visual molecular dynamics) software.[50]

CuOOH-supported reactions by CYP2C9-R125L or CYP2C9.35 enzyme variants that were inactive in the presence of NADPH (Figure 3a and Supplementary Figure S1). Interestingly, the CYP2C9-R125L activity levels were comparable with those of CYP2C9.2 and CYP2C9.1, whereas corresponding rates for CYP2C9.35 were lower apparently because of the potential additive effect of both mutations. Similar results were observed with diclofenac (Figure 3b and Supplementary Figure S2). However, there was a difference in the relative efficiency of CuOOH-dependent catalytic activity of CYP2C9.35 and CYP2C9-R125L toward warfarin as compared with diclofenac (Figure 3). This might be inherent in some structural characteristics of these variant proteins affecting binding of warfarin but not diclofenac. In addition, also hydrogen peroxide (10 mM) was able to support the CYP2C9.35 catalytic activity, albeit with lower efficiency (results not shown). These data clearly indicate that the substrate interactions with these variant enzymes are not altered, suggesting impaired electron transfer from POR to CYP2C9.35.

In silico analysis of Arg125Leu role in CYP2C9-POR interaction

In silico structural analysis of CYP2C9, carrying either Arg125Leu or Arg125Leu/Arg144Cys amino-acid changes, has been carried out to provide a detailed explanation of the structural/functional

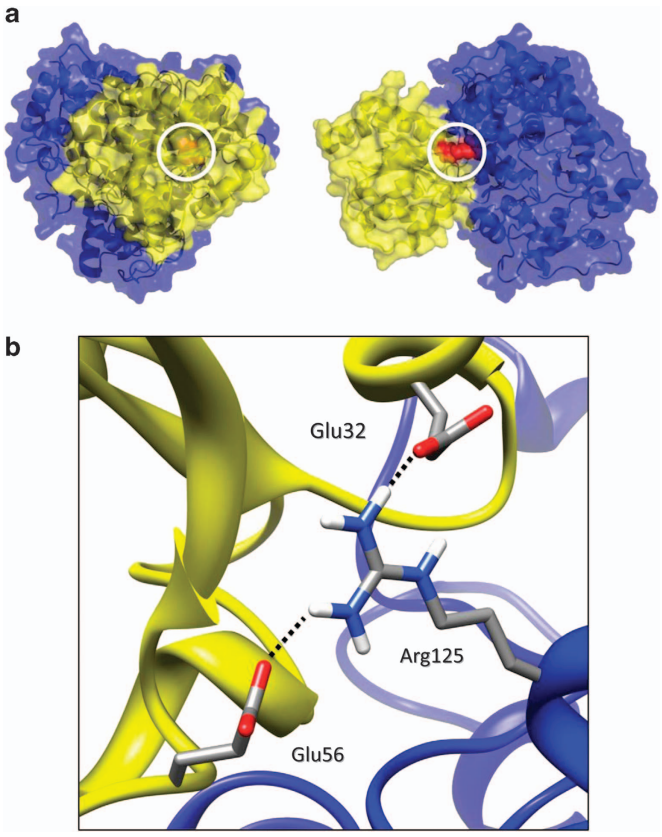

Figure 5. Protein–protein docking model and salt bridges altered in the CYP2C9-R125L and flavine mononucleotide (FMN)-binding domain of CYP oxidoreductase (POR) interaction. (**a**). The complex between CYP2C9 and the FMN-binding domain of POR is shown in two different orientations with the surface of the FMN-binding domain highlighted in yellow and that of the CYP2C9, in blue. The white circle encloses the Arg125 residue that is represented by a spacefill model colored in red. (**b**) Close view of the salt bridges between Arg125 and glutamic acid residues 32 and 56 in the CYP2C9.1-FMN complex. The image was generated using the Chimera software.[28] CYP2C9, cytochrome P450 2C9.

effects produced by the Arg125Leu mutation. Figure 4a represents a cartoon style structural model of all three CYP2C9 variants based on the available 3D structure of CYP2C9 (PDB ID: 1OG2). Calculation of the electrostatic surface showed considerably smaller positive potential area above the helix C of CYP2C9-R125L as compared with CYP2C9.1 (Figure 4b). At the same time, the electrostatic potential of the region representing the access channel of the incoming substrate that involves loops between helices B and C and helices F and G[13] is identical in the mutant and wild-type CYP2C9 variants (Figure 4c).

It was earlier shown that the surface locus of many CYPs, having a number of positively charged amino acids, for example, arginines, corresponding to the Arg125 in CYP2C9, are involved in CYP-POR interactions.[36,37] To analyze the effect of the Arg125Leu/Arg144Cys amino-acid changes on this interaction, a model of CYP2C9[13] complexed with the FMN-binding domain of POR[26] has been built using the complex between the CYP- and FMN-binding domain of POR from *Bacillus megaterium* as a template.[27] The resulting model indicates that the CYP2C9 surface region containing Arg125, with an altered electrostatic potential surface in the CYP2C9-R125L (Figure 4), is involved in the interaction with the FMN-binding domain of POR (Figure 5a). Further refinement of this model with protein–protein docking showed that Arg125 strongly contributes to the stabilization of heterodimeric complex where it is directly involved in the formation of two salt bridges with Glu32 and Glu56 of the FMN-binding domain (Figure 5b). Analysis of the electrostatic potential distribution on the two interacting surfaces indicates high electrostatic complementarity (Supplementary Figure S3). However, in the Arg125Leu variant the electrostatic complementarity and the salt bridges are lost, suggesting a reduced ability of interaction with the FMN-binding domain.

DISCUSSION

We have recently reported a novel CYP2C9-R125L/R144C polymorphism found in a warfarin hypersensitive patient,[21] which was defined as the new *CYP2C9*35* allele. The hypothesis was put forward that the warfarin hypersensitivity might be explained by the reduced metabolic capacity of CYP2C9 due to the amino-acid exchanges. Indeed, here we showed that the expression of CYP2C9 variants containing Arg125Leu and Arg125Leu/Arg144Cys substitutions led to the enzyme inactivation in the NADPH-dependent reactions. We have previously proposed[21] that the apparent lack of *in vivo* activity of CYP2C9.35 might be connected with impaired interaction between CYP2C9 and POR. The finding that CYP2C9.35 was capable to hydroxylate both *S*-warfarin and diclofenac in CuOOH-supported reactions indicate that this indeed is the case. In addition, the structural models presented here suggest a rearrangement of electrostatic surface of the proximal locus in CYP2C9-R125 as an underlying mechanism for the impaired CYP-POR interactions.

Arginine at the position 125 in CYP2C9 is one of the key residues that has been discussed for long time as one of the functional binding sites of P450 enzymes with their redox partners, such as cytochrome b_5 (cyt b_5) and POR.[38] Arg125 is strongly conserved not only between the human CYP2 family members but also with homologous CYPs from mouse (CYP2A5) and rabbit (CYP2B4) (Figure 6). Thus, in CYP2A5, mutation of the corresponding residue, Arg129, to serine decreased the ability of CYP2A5 to bind to cyt b_5-conjugated Sepharose 4B.[39] In CYP2B4, six mostly basic residues corresponding to residues Lys121-Lys138 in CYP2C9 (Figure 6) and, in addition Arg433, were suggested as candidate amino acids for binding to cyt b_5 and POR.[37,40–42] Bridges *et al.*[37] mutated several hydrophobic and basic solvent-exposed amino acids of CYP2B4 including Arg126 (Figure 6) that is located in the mobile C-helix on the proximal surface of CYP2B4[36] and found decreased metabolism of methoxyflurane in the presence of POR. Although substrates could bind normally to these mutant proteins, the interactions with both POR and cyt b_5 were drastically decreased with the increase in the dissociation constant between the interacting partners by 13- and 22-fold, respectively.[37] However, upon the addition of excess of P450 oxidoreductase to the reaction mixture, the V_{max} returned to control values, indicating that the mutations did not affect the catalytic mechanism *per se* but the binding to redox partners.[37] These mutations are likely to cause local structural and electrostatic perturbations that would contribute to the decrease in the binding of the mutant P450s to cyt b_5.[37]

Our structural analysis confirms and extends this hypothesis. We show that the Arg125Leu amino-acid change strongly contributes to the decrease of electrostatic potential of CYP2C9 proximal surface that is complementary to the corresponding negatively charged surface of FMN-binding domain of POR (Supplementary Figure S3). As shown in Figure 5b, such loss of electrostatic interaction results in the disruption of important salt bridges between the two proteins. This may lead to destabilization of CYP-POR complex and hinder the electron transport between them. This mutation however had no impact on the substrate binding loci of CYP2C9, which suggests that elimination of the positively charged Arg125 cannot perturb the substrate–enzyme interaction.

Another argument in favor of the altered CYP-POR interactions and not the substrate binding site modification is that in the

Figure 6. Alignment of the amino-acid sequences representing the interaction surface of various cytochrome P450s (CYPs) with CYP oxidoreductase (POR). Alignment includes CYPs from human 2C family and the homologous mouse (CYP2A5) and rabbit (CYP2B4) proteins. Identical or similar amino acids suggested to be involved in interaction with POR are highlighted in gray.

presence of NADPH, CYP2C9.35 and CYP2C9-R125L remained catalytically silent with all three substrates used in this study, that is, *S*-warfarin, diclofenac and losartan. It is known that despite the docking of these structurally diverse molecules occurs in the same binding site cavity, their orientation in this channel and interacting amino-acid residues are very different.[13,43–46] Therefore, the conformational impact of Arg125Leu substitution on the substrate binding could unlikely be identical for all of these three molecules.

In addition to Arg125Leu, the CYP2C9.35 variant protein includes an Arg144Cys change. The CYP2C9 variant that contains only this mutation is known as CYP2C9.2 and its expression causes a moderately reduced enzyme activity toward several substrates including warfarin, diclofenac and losartan.[9,11,47] This is in line with our data obtained in the HEK293 cell system showing reduced activity of CYP2C9-R144C toward *S*-warfarin in NADPH-POR-supported system. However, the structural basis for the reduced catalytic activity of CYP2C9-R144C remains elusive. Earlier reports attempted to explain such reduction by the altered interaction between CYP2C9 and POR[12] or differences in spin state of CYP2C9.[48] Our data partially supports the former assumption as in the CuOOH peroxide shunt system the activity of CYP2C9-R144C was restored to CYP2C9.1 levels (results not shown). However, in contrast to Arg125, this residue is not fully solvent exposed and therefore its contribution to the overall positive electrostatic potential of the CYP-POR interacting surface is negligible. It could be speculated that in the CYP2C9-R144C mutant, reactive cysteine might be involved in the fortuitous interactions with POR and/or with other molecular partner, thus reducing the probability of the formation of correct CYP2C9-FMN-binding domain binary complex. Alternatively, it has been suggested that this mutation may interfere with substrate binding via the expansion of the substrate-binding pocket and increased fluctuations of several important residues responsible for substrate holding, as observed in a previous molecular dynamics simulation study.[20]

In conclusion, our data demonstrate that the Arg125Leu change in CYP2C9.35 strongly augments the modest inhibitory effect of the Arg144Cys mutation found in the carriers of *CYP2C9*2* allelic variant. The *in silico* structural as well as the *in vitro* analyses suggest impaired functional CYP2C9-POR interaction as a major molecular mechanism behind such inhibitory effect. Despite the seemingly low population frequency of *CYP2C9*35*, it should be noted that this number could be higher as many subjects identified as a *CYP2C9*2* genotype might also have the additional R125L substitution and therefore may have been misclassified. Thorough genotyping for the presence of both polymorphic changes might therefore facilitate more accurate warfarin dosing using this allele as a specific genetic biomarker.

CONFLICT OF INTEREST

The authors declare no conflict of interest.

ACKNOWLEDGMENTS

We thank Dr Robert J Edward for a kind offer of human anti-CYP2C serum. This work was supported by grants from The Swedish Research Council and from Karolinska Institutet.

REFERENCES

1 Lohr JW, Willsky GR, Acara MA. Renal drug metabolism. *Pharmacol Rev* 1998; **50**: 107–141.
2 Hrycay EG, Gustafsson JA, Ingelman-Sundberg M, Ernster L. Sodium periodate, sodium chloride, organic hydroperoxides, and H_2O_2 as hydroxylating agents in steroid hydroxylation reactions catalyzed by partially purified cytochrome *P*-450. *Biochem Biophys Res Commun* 1975; **66**: 209–216.
3 Barr DP, Martin MV, Guengerich FP, Mason RP. Reaction of cytochrome P450 with cumene hydroperoxide: ESR spin-trapping evidence for the homolytic scission of the peroxide O–O bond by ferric cytochrome P450 1A2. *Chem Res Toxicol* 1996; **9**: 318–325.
4 Rendic S, Di Carlo FJ. Human cytochrome P450 enzymes: a status report summarizing their reactions, substrates, inducers, and inhibitors. *Drug Metab Rev* 1997; **29**: 413–580.
5 Zanger UM, Schwab M. Cytochrome P450 enzymes in drug metabolism: regulation of gene expression, enzyme activities, and impact of genetic variation. *Pharmacol Therap* 2013; **138**: 103–141.
6 Eriksson N, Wadelius M. Prediction of warfarin dose: why, when and how? *Pharmacogenomics* 2012; **13**: 429–440.
7 Johnson JA, Gong L, Whirl-Carrillo M, Gage BF, Scott SA, Stein CM *et al.* Clinical Pharmacogenetics Implementation Consortium Guidelines for CYP2C9 and VKORC1 genotypes and warfarin dosing. *Clin Pharmacol Ther* 2011; **90**: 625–629.
8 Yin T, Miyata T. Warfarin dose and the pharmacogenomics of CYP2C9 and VKORC1—rationale and perspectives. *Thromb Res* 2007; **120**: 1–10.
9 Yasar U, Eliasson E, Forslund-Bergengren C, Tybring G, Gadd M, Sjoqvist F *et al.* The role of CYP2C9 genotype in the metabolism of diclofenac *in vivo* and *in vitro*. *Eur J Clin Pharmacol* 2001; **57**: 729–735.
10 Yasar U, Forslund-Bergengren C, Tybring G, Dorado P, Llerena A, Sjoqvist F *et al.* Pharmacokinetics of losartan and its metabolite E-3174 in relation to the CYP2C9 genotype. *Clin Pharmacol Ther* 2002; **71**: 89–98.
11 Rokitta D, Fuhr U. Comparison of enzyme kinetic parameters obtained *in vitro* for reactions mediated by human CYP2C enzymes including major CYP2C9 variants. *Curr Drug Metab* 2010; **11**: 153–161.
12 Crespi CL, Miller VP. The R144C change in the CYP2C9*2 allele alters interaction of the cytochrome P450 with NADPH:cytochrome P450 oxidoreductase. *Pharmacogenetics* 1997; **7**: 203–210.
13 Williams PA, Cosme J, Ward A, Angove HC, Matak Vinkovic D, Jhoti H. Crystal structure of human cytochrome P450 2C9 with bound warfarin. *Nature* 2003; **424**: 464–468.
14 Wester MR, Yano JK, Schoch GA, Yang C, Griffin KJ, Stout CD *et al.* The structure of human cytochrome P450 2C9 complexed with flurbiprofen at 2.0-A resolution. *J Biol Chem* 2004; **279**: 35630–35637.
15 Hata M, Hirano Y, Hoshino T, Tsuda M. Monooxygenation mechanism by cytochrome *p*-450. *J Am Chem Soc* 2001; **123**: 6410–6416.
16 Hata M, Tanaka Y, Kyoda N, Osakabe T, Yuki H, Ishii I *et al.* An epoxidation mechanism of carbamazepine by CYP3A4. *Bioorg Med Chem* 2008; **16**: 5134–5148.
17 Li W, Liu H, Scott EE, Grater F, Halpert JR, Luo X *et al.* Possible pathway(s) of testosterone egress from the active site of cytochrome P450 2B1: a steered molecular dynamics simulation. *Drug Metab Dispos* 2005; **33**: 910–919.
18 Li W, Liu H, Luo X, Zhu W, Tang Y, Halpert JR *et al.* Possible pathway(s) of metyrapone egress from the active site of cytochrome P450 3A4: a molecular dynamics simulation. *Drug Metab Dispos* 2007; **35**: 689–696.
19 Li W, Tang Y, Liu H, Cheng J, Zhu W, Jiang H. Probing ligand binding modes of human cytochrome P450 2J2 by homology modeling, molecular dynamics simulation, and flexible molecular docking. *Proteins* 2008; **71**: 938–949.
20 Sano E, Li W, Yuki H, Liu X, Furihata T, Kobayashi K *et al.* Mechanism of the decrease in catalytic activity of human cytochrome P450 2C9 polymorphic variants investigated by computational analysis. *J Comput Chem* 2010; **31**: 2746–2758.
21 Ciccacci C, Falconi M, Paolillo N, Oteri F, Forte V, Novelli G *et al.* Characterization of a novel CYP2C9 gene mutation and structural bioinformatic protein analysis in a warfarin hypersensitive patient. *Pharmacogenet Genom* 2011; **21**: 344–346.

22 Bradford MM. A rapid and sensitive method for the quantitation of microgram quantities of protein utilizing the principle of protein–dye binding. *Anal Biochem* 1976; **72**: 248–254.
23 Edwards RJ, Adams DA, Watts PS, Davies DS, Boobis AR. Development of a comprehensive panel of antibodies against the major xenobiotic metabolising forms of cytochrome P450 in humans. *Biochem Pharmacol* 1998; **56**: 377–387.
24 Lang D, Bocker R. Highly sensitive and specific high-performance liquid chromatographic analysis of 7-hydroxywarfarin, a marker for human cytochrome *P*-4502C9 activity. *J Chromatogr B* 1995; **672**: 305–309.
25 Inoue T, Nitta K, Sugihara K, Horie T, Kitamura S, Ohta S. CYP2C9-catalyzed metabolism of *S*-warfarin to 7-hydroxywarfarin *in vivo* and *in vitro* in chimeric mice with humanized liver. *Drug Metab Dispos* 2008; **36**: 2429–2433.
26 Zhao Q, Modi S, Smith G, Paine M, McDonagh PD, Wolf CR *et al.* Crystal structure of the FMN-binding domain of human cytochrome P450 reductase at 1.93 A resolution. *Protein Sci* 1999; **8**: 298–306.
27 Sevrioukova IF, Li H, Zhang H, Peterson JA, Poulos TL. Structure of a cytochrome P450-redox partner electron-transfer complex. *Proc Natl Acad Sci USA* 1999; **96**: 1863–1868.
28 Pettersen EF, Goddard TD, Huang CC, Couch GS, Greenblatt DM, Meng EC *et al.* UCSF Chimera—a visualization system for exploratory research and analysis. *J Comput Chem* 2004; **25**: 1605–1612.
29 Hubbard SJ, Thornton JM, Campbell SF. Substrate recognition by proteinases. *Faraday Discuss* 1992; **93**: 13–23.
30 Dominguez C, Boelens R, Bonvin AM. HADDOCK: a protein–protein docking approach based on biochemical or biophysical information. *J Am Chem Soc* 2003; **125**: 1731–1737.
31 Dolinsky TJ, Nielsen JE, McCammon JA, Baker NA. PDB2PQR: an automated pipeline for the setup of Poisson–Boltzmann electrostatics calculations. *Nucleic Acids Res* 2004; **32**: W665–W667.
32 Wang JCP, Kollman PA. How well does a restrained electrostatic potential (RESP) model perform in calculating conformational energies of organic and biological molecules? *J Comput Chem* 2000; **21**: 1049–1074.
33 Oda A, Yamaotsu N, Hirono S. New AMBER force field parameters of heme iron for cytochrome P450s determined by quantum chemical calculations of simplified models. *J Comput Chem* 2005; **26**: 818–826.
34 Baker NA, Sept D, Joseph S, Holst MJ, McCammon JA. Electrostatics of nanosystems: application to microtubules and the ribosome. *Proc Natl Acad Sci USA* 2001; **98**: 10037–10041.
35 Hrycay EG, Gustafsson JA, Ingelman-Sundberg M, Ernster L. The involvement of cytochrome P-450 in hepatic microsomal steroid hydroxylation reactions supported by sodium periodate, sodium chlorite, and organic hydroperoxides. *Eur J Biochem* 1976; **61**: 43–52.
36 Hasemann CA, Kurumbail RG, Boddupalli SS, Peterson JA, Deisenhofer J. Structure and function of cytochromes P450: a comparative analysis of three crystal structures. *Structure* 1995; **3**: 41–62.
37 Bridges A, Gruenke L, Chang YT, Vakser IA, Loew G, Waskell L. Identification of the binding site on cytochrome P450 2B4 for cytochrome b5 and cytochrome P450 reductase. *J Biol Chem* 1998; **273**: 17036–17049.
38 Im SC, Waskell L. The interaction of microsomal cytochrome P450 2B4 with its redox partners, cytochrome P450 reductase and cytochrome *b*(5). *Arch Biochem Biophys* 2011; **507**: 144–153.
39 Juvonen RO, Iwasaki M, Negishi M. Roles of residues 129 and 209 in the alteration by cytochrome *b*5 of hydroxylase activities in mouse 2A P450S. *Biochemistry* 1992; **31**: 11519–11523.
40 Omata Y, Robinson RC, Gelboin HV, Pincus MR, Friedman FK. Specificity of the cytochrome *P*-450 interaction with cytochrome *b*5. *FEBS Lett* 1994; **346**: 241–245.
41 Omata Y, Sakamoto H, Robinson RC, Pincus MR, Friedman FK. Interaction between cytochrome P450 2B1 and cytochrome *bs*: inhibition by synthetic peptides indicates a role for P450 residues Lys-122 and Arg-125. *Biochem Biophys Res Commun* 1994; **201**: 1090–1095.
42 Davydov DR, Darovsky BV, Dedinsky IR, Kanaeva IP, Bachmanova GI, Blinov VM *et al.* Cytochrome *C* (Fe^{2+}) as a competitive inhibitor of NADPH-dependent reduction of cytochrome P450 LM2: locating protein–protein interaction sites in microsomal electron carriers. *Arch Biochem Biophys* 1992; **297**: 304–313.
43 Wester MR, Johnson EF, Marques-Soares C, Dijols S, Dansette PM, Mansuy D *et al.* Structure of mammalian cytochrome P450 2C5 complexed with diclofenac at 2.1 A resolution: evidence for an induced fit model of substrate binding. *Biochemistry* 2003; **42**: 9335–9345.
44 Klose TS, Ibeanu GC, Ghanayem BI, Pedersen LG, Li L, Hall SD *et al.* Identification of residues 286 and 289 as critical for conferring substrate specificity of human CYP2C9 for diclofenac and ibuprofen. *Arch Biochem Biophys* 1998; **357**: 240–248.
45 Haining RL, Jones JP, Henne KR, Fisher MB, Koop DR, Trager WF *et al.* Enzymatic determinants of the substrate specificity of CYP2C9: role of B′–C loop residues in providing the pi-stacking anchor site for warfarin binding. *Biochemistry* 1999; **38**: 3285–3292.
46 Melet A, Assrir N, Jean P, Pilar Lopez-Garcia M, Marques-Soares C, Jaouen M *et al.* Substrate selectivity of human cytochrome P450 2C9: importance of residues 476, 365, and 114 in recognition of diclofenac and sulfaphenazole and in mechanism-based inactivation by tienilic acid. *Arch Biochem Biophys* 2003; **409**: 80–91.
47 Sullivan-Klose TH, Ghanayem BI, Bell DA, Zhang ZY, Kaminsky LS, Shenfield GM *et al.* The role of the CYP2C9-Leu359 allelic variant in the tolbutamide polymorphism. *Pharmacogenetics* 1996; **6**: 341–349.
48 Wei L, Locuson CW, Tracy TS. Polymorphic variants of CYP2C9: mechanisms involved in reduced catalytic activity. *Mol Pharmacol* 2007; **72**: 1280–1288.
49 Mkrtchian S, Sandalova T. ERp29, an unusual redox-inactive member of the thioredoxin family. *Antioxid Redox Signal* 2006; **8**: 325–337.
50 Humphrey W, Dalke A, Schulten K. VMD: visual molecular dynamics. *J Mol Graph* 1996; **141:** 27–38.

Supplementary Information accompanies the paper on the The Pharmacogenomics Journal website (http://www.nature.com/tpj)